IL NUOVO CIMENTO Vol. 28 C, N. 6 Novembre-Dicembre 2005
DOI 10.1393/ncc/i2005-10134-1

On the computation of the Benjamin-Feir Index(*)

M. Serio(1), M. Onorato(1), A. R. Osborne(1) and P. A. E. M. Janssen(2)
(1) *Dipartimento di Fisica Generale, Università di Torino*
Via P. Giuria, 1 - 10125 Torino, Italy
(2) *European Centre for Medium-Range Weather Forecasts*
Reading RG2 9AX, Berks, England

(ricevuto l' 11 Luglio 2005; approvato il 19 Luglio 2005; pubblicato online il 19 Dicembre 2005)

Summary. — Recently it has been shown theoretically, numerically and experimentally that the statistical properties (probability density function of wave amplitude and wave height) of long crested surface gravity waves depend not only on steepness but also on the Benjamin-Feir Index (BFI), which is the ratio between wave steepness and spectral bandwidth. The computation of this index requires the estimation of a number of parameters such as the spectral bandwidth and the peak frequency. For a given time series or a wave spectrum those parameters can be calculated using different methods, thus leading to different numerical values of the BFI. We analyze different approaches for computing the BFI and, based on numerical experiments with simulated spectra, we outline a unique robust methodology for its computation.

PACS 92.10.Hm – Surface waves, tides, and sea level.
PACS 47.35.+i – Hydrodynamic waves.

1. – Introduction

It is well known that a Stokes wave in deep water is unstable to suitable small amplitude long perturbations. If a_0 is the Stokes amplitude and k_0 is its wave number, then the wave is unstable whenever ak_0 is greater than $K/(2\sqrt{2}k_0)$, where K is the wave number of the perturbation. This instability, well known in other fields of physics as the modulational instability, is known in the field of surface gravity waves as the Benjamin-Feir instability. The effect of this instability is the following: as the Stokes wave becomes unstable, a single wave in the middle of the group begins to grow at the expense of the surrounding waves (actually borrowing mass from them), giving rise to a large amplitude wave. Recently it has been shown theoretically [1], numerically [2-4] and experimentally [5-7] that, if the wave steepness is sufficiently large and the spectral bandwidth is sufficiently small, this effect can take place also in a random spectra.

(*) The authors of this paper have agreed to not receive the proofs for correction.

As a consequence of this instability the statistical properties of the surface elevation, for example the kurtosis, have been found to be different from the expected Gaussian values. Deviations from the Gaussian predictions are more pronounced if the ratio of the steepness and spectral bandwidth, known as the Benjamin-Feir Index (BFI) [1, 3], is large. Therefore, the BFI has become a parameter that characterizes the statistical properties of surface gravity waves.

The simplest and probably the most instructive way to introduce formally the Benjamin-Feir Index is to start with the Nonlinear Schroedinger equation (see for example [2]). Note that, even though we will define the BFI using the Nonlinear Schroedinger (NLS) equation, the dependence of the statistical properties of the surface gravity waves does not rely on the fact that it has been derived from the NLS equation. The NLS equation represents a perfect framework in which only the basic features of the modulational instability are contained. The equation is a weakly nonlinear, narrow-banded approximation of the fully nonlinear irrotational and inviscid water wave equations. It is the result of the balance between nonlinearity and dispersion and it has the following form:

$$\frac{\partial A}{\partial t} + \frac{1}{2}\frac{\omega_0}{k_0}\nu\frac{\partial A}{\partial x} + i\frac{1}{8}\frac{\omega_0}{k_0^2}\,\alpha\frac{\partial^2 A}{\partial x^2} + i\frac{1}{2}\omega_0 k_0^2\beta\, A\,|A|^2 = 0\,,$$

where A is the complex wave envelope, ν is the correction to the group velocity for finite depth, α and β are coefficients that in general depend on the water depth, h, on the dominant wave number, k_0, and the corresponding angular frequency, ω_0. The general forms of ν, α and β for arbitrary depth are here reported (see [8] for the derivation):

$$\nu = 1 + 2\frac{k_0 h}{\sinh(2k_0 h)}\,,$$

$$\alpha = -\nu^2 + 2 + 8(k_0 h)^2\frac{\cosh(2k_0 h)}{\sinh^2(2k_0 h)}\,,$$

$$\beta = \frac{\cosh(4k_0 h) + 8 - 2\tanh^2(k_0 h)}{8\sinh^4(k_0 h)} - \frac{\left(2\cosh^2(k_0 h) + 0.5\nu\right)^2}{\sinh^2(2k_0 h)\left[\frac{k_0 h}{\tanh(k_0 h)} - \left(\frac{\nu}{2}\right)^2\right]}\,.$$

In order to derive the BFI we use the standard procedure used to derive for example the Reynolds number from the Navier-Stokes equation, *i.e.* we write the equation in non-dimensional form introducing the following non-dimensional quantities:

$$A' = \frac{A}{a}\,, \qquad x' = \Delta k x\,, \qquad t' = \frac{\omega_0 \Delta k^2 \alpha}{8k_0^2}t\,.$$

Here Δk corresponds to a measure of the spectral bandwidth and has the dimensions of 1/length. Primes denote non-dimensional variables. In a frame of reference moving with the group velocity the non-dimensional NLS equation becomes (primes have been now omitted for brevity)

$$\frac{\partial A}{\partial t} + i\frac{\partial^2 A}{\partial x^2} + i\left(\frac{2\varepsilon}{\Delta k/k_0}\right)^2\frac{\beta}{\alpha}\,A\,|A|^2 = 0\,,$$

where $\varepsilon = k_0 a$ is the wave steepness. We define the Benjamin-Feir Index as the square root of the coefficient that multiplies the nonlinear term:

$$\mathrm{BFI} = \frac{2\varepsilon}{\Delta k/k_0}\sqrt{\frac{|\beta|}{\alpha}}\,.$$

The ratio β/α tends to one as $k_0 h$ tends to infinity and decreases as the water depth decreases, becoming negative for values of $k_0 h$ smaller than 1.36. In such a case the modulational instability disappears and Stokes waves are stable to perturbations. Note that if time series (or frequency spectra) are available the following definition should be used:

$$\mathrm{BFI} = \frac{\varepsilon}{\Delta\omega/\omega_0}\nu\sqrt{\frac{|\beta|}{\alpha}}\,, \tag{1}$$

where we have used the fact that

$$\frac{\Delta\omega}{\omega_0} = \frac{\nu}{2}\frac{\Delta k}{k_0}\,.$$

The methodology of computation of the BFI is unique when a Stokes wave is considered: the characteristic amplitude, a, of the Stokes wave is the amplitude itself and the spectral bandwidth corresponds to the wave number of the perturbation considered. Here our goal is to compute the BFI from random waves; therefore the parameters involved in the definition of the BFI must be estimated from the time series or wave spectrum. For random waves such as for example those characterized by the JONSWAP spectrum, the computation of the BFI is not univocally defined, in the sense that different methodologies can be used to estimate the wave steepness, the spectral bandwidth and the dominant frequency. In the next section we will analyze critically different methodologies for the computation of the BFI and as a result of the analysis a unique definition of the BFI for single-peaked spectra will be given.

An alternative approach is to focus on the mathematical and physical structure of NLS and to analyze data from the point of view of the inverse scattering transform solution of the equation [7]. In this approach the application of multidimensional Fourier methods provides a unique and valuable estimate of the BFI, together with many other properties of the wave train, including the unique determination of the "unstable modes" or "rogue wave" basis function in a measured wave train. We have addressed a number of aspects of this method in Osborne *et al.* [7].

2. – Estimation of BFI for random waves

The two parameters that are involved in the computation of BFI are the wave steepness and the spectral bandwidth. The steepness requires an estimation of characteristic wave amplitude and a dominant wave number. The wave amplitude can be estimated as follows:

$$a = \frac{H_{m_0}}{2\sqrt{2}} = \sqrt{2m_0}\,, \tag{2}$$

where

$$m_0 = \int_0^\infty P(f)\, \mathrm{d}f \tag{3}$$

with $P(f)$ the wave spectral density function. Note that for a sinusoidal wave the use of the definition in eq. (2) leads exactly to the wave amplitude. To evaluate the steepness it is also necessary to determine the peak frequency and then use the linear dispersion relation to obtain the dominant wave number. Due to the statistical variability of the spectral estimate and the discrete frequency resolution of the spectra, the peak frequency can be considered a stochastic variable. A number of techniques have been proposed for its computation and of the confidence interval [9-12]. Young [13] has critically reviewed these proposals and found that the most reliable technique involves the use of a weighted integral of the form of

$$\hat{f}_\mathrm{p} = \frac{\int_0^\infty f\, P^4(f)\, \mathrm{d}f}{\int_0^\infty P^4(f)\, \mathrm{d}f}\,, \tag{4}$$

$\hat{f}_\mathrm{p}$ is an estimate of the true peak frequency f_p. Young found that the computation based on eq. (4), as other techniques, slightly overestimates the value of f_p and showed that the 95% confidence limits (which depend on the number of degree of freedom of the spectral estimate and on the spectral resolution) determined from (4) are

$$a_\mathrm{l}\hat{f}_\mathrm{p} \leqslant f_\mathrm{p} \leqslant a_\mathrm{u}\hat{f}_\mathrm{p}\,,$$

where a_l and a_u are factors defining the lower and upper 95% confidence limits, respectively. For a given spectral resolution, the a_l and a_u factors evaluated by Young remain practically constant for a number of degree of freedom greater than 50.

Once the dominant frequency (dominant wave number) and the characteristic amplitude have been computed, the wave steepness can be univocally determined. The next step is the estimation of the spectral bandwidth. The simplest way to do this is to calculate the half-width at half-maximum of the wave spectrum, although it turns out that the method is not robust especially if one deals with "noisy spectra"; therefore methods based on integral properties of the wave spectrum are definitely preferred. In the literature a number of methods to characterize the spectral bandwidth have been introduced in the past. We will consider three of them that are defined in Goda's book [14]; the book contains a comprehensive list of parameters used for characterizing field and laboratory surface gravity waves (we will use the same nomenclature as in the book). Before giving the definition of these parameters we will define the spectral moments in the following way:

$$m_i = \int_0^\infty f^i P(f)\, \mathrm{d}f\,.$$

The first estimation of the spectral bandwidth is the so-called broadness parameter defined as

$$\sigma_{\mathrm{B}} = \sqrt{1 - \frac{m_2^2}{m_0 m_4}}\,. \tag{5}$$

It was introduced by Cartwright and Longuet-Higgins [15]. A spectrum is considered to be narrow banded if s_{B} tends to zero. The second method was again introduced by Longuet-Higgins [16] and is known as the narrowness parameter

$$\sigma_{\mathrm{N}} = \sqrt{\frac{m_0 m_2}{m_1^2} - 1}\,. \tag{6}$$

The last definition that we will consider to be the peakedness parameter (or quality factor) that was introduced by Goda [17]:

$$Q_{\mathrm{p}} = \frac{2}{m_0^2} \int_0^\infty f P^2(f) \mathrm{d}f\,. \tag{7}$$

2˙1. *Application to a Gaussian spectrum.* – In order to have some feeling about the relationship between these parameters, we apply the above definitions to an ideal Gaussian spectrum:

$$P\,(f) = \frac{1}{\sigma\sqrt{2\pi}} \exp\left[-\frac{(f - f_{\mathrm{p}})^2}{2\sigma^2}\right]$$

for which its width and frequency peak are well defined. For a Gaussian spectrum the half-width at half-maximum Δ is related to σ in the following way:

$$\Delta = \sigma\sqrt{2\log(2)} \approx 1.18\sigma\,. \tag{8}$$

It can be shown that the narrowness parameter is related to σ by this simple relation: $\sigma_{\mathrm{N}} = \sigma/f_{\mathrm{p}}$, *i.e.* the narrowness. For the broadness parameter the relation is more involved, nevertheless for small ratio of σ/f_{p}, the broadness parameter and the narrowness parameter are related as follows:

$$\sigma_{\mathrm{N}} = \frac{\sigma}{f_{\mathrm{p}}} \approx \frac{1}{2}\sigma_{\mathrm{B}}\,. \tag{9}$$

Concerning the quality factor, we find the following:

$$Q_{\mathrm{p}} = \frac{f_{\mathrm{p}}}{2\sqrt{\pi}\sigma}\left(1 + \mathrm{Erf}\left[\frac{f_{\mathrm{p}}}{\sigma}\right]\right) + \frac{\exp\left[-\left(f_{\mathrm{p}}/\sigma\right)^2\right]}{2\pi} \approx \frac{f_{\mathrm{p}}}{\sqrt{\pi}\sigma}\,. \tag{10a}$$

The last relation is obtained in the case of small σ/f_{p}. Using the previous relations, the peakedness parameter can be related to the narrowness parameter (or the broadness

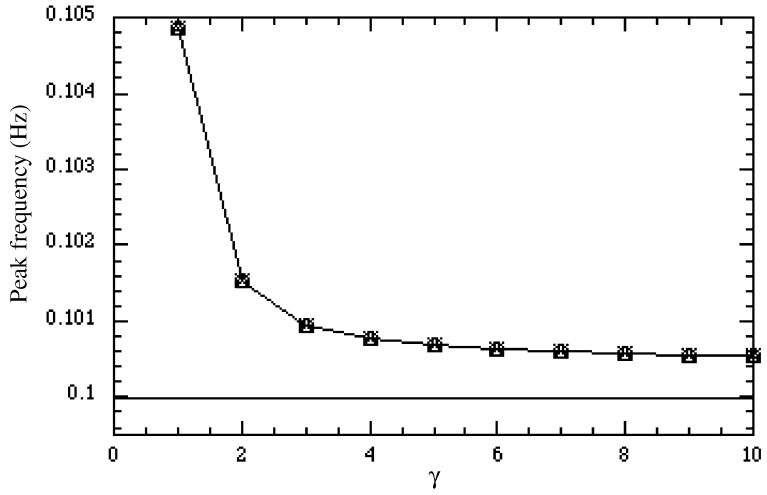

Fig. 1. – Estimated dominant frequency as a function of the enhancement parameter for three different maximum frequencies (crosses correspond to $f_{\max} = 8f_{\mathrm{p}}$, triangles to $f_{\max} = 4f_{\mathrm{p}}$, circles to $f_{\max} = 3f_{\mathrm{p}}$). The solid line is relative to the value used in the generation of the power spectrum.

parameter) for a narrow Gaussian spectrum in the following way:

$$Q_{\mathrm{p}} \approx \frac{1}{\sigma_{\mathrm{N}}\sqrt{\pi}} \approx \frac{2}{\sigma_{\mathrm{B}}\sqrt{\pi}}\,. \tag{10b}$$

Note also that using eq. (8) the quality factor can be related to half-width at half-maximum of the spectrum:

$$Q_{\mathrm{p}} \approx \frac{f_{\mathrm{p}}}{\sqrt{\pi}\Delta}\sqrt{2\log(2)}\,. \tag{10c}$$

In the next section those methods will be applied to a simulated JONSWAP spectra and the results on the computation of the BFI index will be discussed. We anticipate that, as explained for example in [14], the value of the narrowness (or broadness parameter) for a real sea state is very sensitive to the tail of the spectrum and to the cut-off frequency, therefore the quality factor seems to be a better choice for an estimate of the spectral bandwidth for a realistic data set. This aspect will be discussed in the following section.

3. – BFI for numerically simulated JONSWAP spectrum

We consider the classical form of the JONSWAP spectrum (see, *e.g.*, [18]):

$$P(f) = \frac{\alpha}{f^5}\exp\left[-\frac{5}{4}\left(\frac{f_{\mathrm{p}}}{f}\right)^4\right]\gamma^{\exp\left[-\frac{(f-f_{\mathrm{p}})^2}{2\sigma_0^2 f_{\mathrm{p}}^2}\right]} \qquad \begin{matrix}\sigma_0 = 0.07 & f \leqslant f_{\mathrm{p}}\,,\\ \sigma_0 = 0.09 & f \geqslant f_{\mathrm{p}}\,.\end{matrix} \tag{11}$$

The parameters α, γ and σ_0 were originally obtained by fitting experimental data from the international JONSWAP experiment conducted during 1968-69 in the North

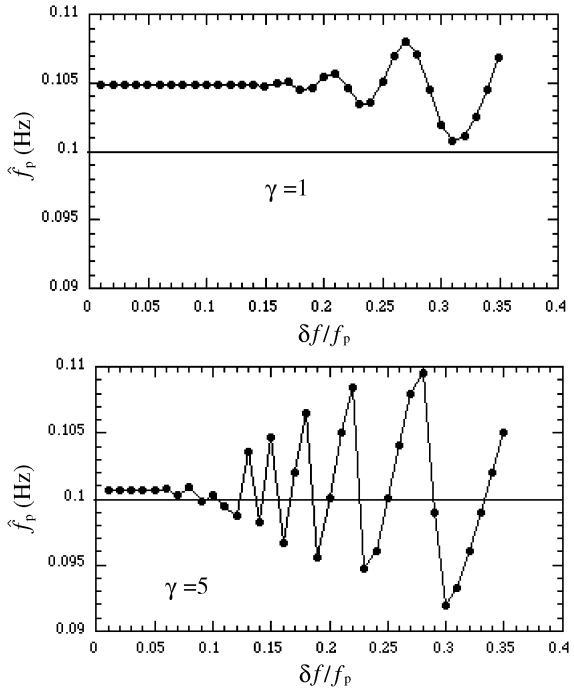

Fig. 2. – Estimate $\hat{f}_{\mathrm{p}}$ of the peak frequency as a function of $\delta f/f_{\mathrm{p}}$ for $\gamma = 1$ (top panel) and $\gamma = 5$ (bottom panel): the solid line is relative to the value used in the generation of the power spectrum.

Sea. Here f_{p} is the peak frequency, γ is the "enhancement" factor and α is the Phillips parameter. Those parameters depend on the stage of the wave development. We here fix, without loss of generality, the peak of the spectrum at 0.1 Hz, the Phillips parameter is taken to be 0.0081 and σ_0 takes on the standard values reported in relation (11). We then change the enhancement parameter, γ, from 1 to 10, the cut-off frequency, $f_{\max}$, from $3f_{\mathrm{p}}$ to $8f_{\mathrm{p}}$, and the relative spectral resolution from $\delta f/f_{\mathrm{p}} = 0.01$ to $\delta f/f_{\mathrm{p}} = 0.5$, here δf is the spectral resolution.

We compute the peak frequency using relation (4); the aim is to quantify the overestimation of f_{p} discussed by Young. Figure 1 reports the values of $\hat{f}_{\mathrm{p}}$ as a function of the enhancement parameter for three different cut-off frequencies: the solid line is relative to the value used in the generation of the power spectrum. As the values of γ increase (and the peak becomes more defined), the overestimation of f_{p} decreases from 5×10^{-2} to 5×10^{-3}. Practically speaking for $\gamma \geqslant 3$ the overestimation of the dominant frequency is lower than the 95% confidence intervals and this behavior is independent of the number of degree of freedom considered.

The effects of the spectral resolution on the determination of the spectral peak are more drastic. For the various values of the enhancement parameter γ we observe that the estimated $\hat{f}_{\mathrm{p}}$ remains constant only in a limited range of the spectral resolution. Figure 2 shows $\hat{f}_{\mathrm{p}}$ as a function of $\delta f/f_{\mathrm{p}}$ for $\gamma = 1$ (top panel) and $\gamma = 5$ (bottom panel): there are clear fluctuations that reach 20% of the true f_{p} value, a limit greater than the expected confidence interval. By considering at the same time the values of γ, the range of

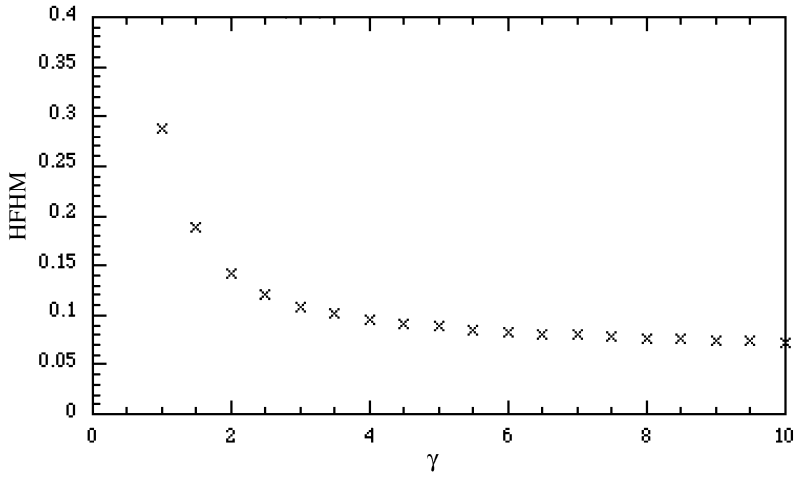

Fig. 3. – Behavior of the half-width at half-maximum (HFHM) as a function of γ for the JONSWAP spectrum.

oscillations in the estimate $\hat{f}_{\mathrm{p}}$ and the confidence interval (which is maximum for $\gamma = 1$), we conclude that a reliable estimate of f_{p} requires that $\delta f / f_{\mathrm{p}} \leqslant 0.15$, independently of γ (at least for the values here considered). In this case, from [13], the confidence interval is given by

$$\gamma = 1: \quad 0.97\hat{f}_{\mathrm{p}} \leqslant f_{\mathrm{p}} \leqslant 1.16\hat{f}_{\mathrm{p}} \qquad \text{and} \qquad \gamma > 1: \quad 0.95\hat{f}_{\mathrm{p}} \leqslant f_{\mathrm{p}} \leqslant 1.06\hat{f}_{\mathrm{p}}\,.$$

We now estimate the spectral width. As a first estimation we show in fig. 3 the half-width at half-maximum for the JONSWAP spectrum. The spectral bandwidth decreases as γ increases, especially in the transition $\gamma = 1$ to $\gamma = 2$. We consider fig. 3 as a reference to compare with the other methods previously defined. Our aim is to select a robust methodology insensitive to the cut-off frequency that shows a trend similar to the one observed in fig. 3. We have evaluated the broadness factor σ_{B}, the narrowness factor σ_{N} and the reciprocal of peakedness parameter Q_{p} with three different values of the cut-off frequency: $3f_{\mathrm{p}}$, $4f_{\mathrm{p}}$, $8f_{\mathrm{p}}$. The results are shown in fig. 4. The peakedness factor Q_{p} assumes almost the same value, independent of the cut-off frequency, while the two other parameters decrease with the cut-off frequency, with a relative decrement of the 21% for σ_{N} and 26% for σ_{B} for the greater enhancement parameter. Moreover, while σ_{N} and σ_{B} decrease much slower with respect to the trend shown in fig. 3, $1/Q_{\mathrm{p}}$ seems to better reproduce the behaviour of the half-width at half-maximum. Studying the influence of the spectral resolution on Q_{p} estimates, we find results similar to those obtained for the frequency peak: with a spectral resolution of 0.15, the relative error on Q_{p} reaches the maximum value of 4% for the largest γ.

According to the results just shown, using (1), (2) and (10b) we propose that the BFI be computed from time series (or from frequency spectra) using the following formula:

$$\mathrm{BFI} = \sqrt{m_0}\hat{k}_{\mathrm{p}} Q_{\mathrm{p}} \sqrt{2\pi}\nu \sqrt{\frac{|\beta|}{\alpha}}\,. \tag{12}$$

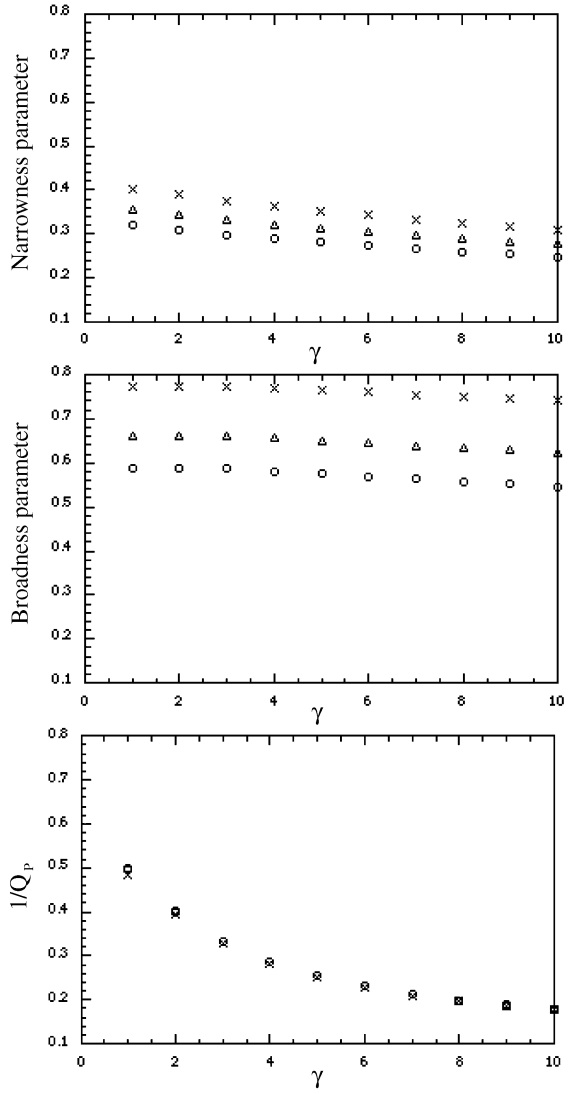

Fig. 4. – Behavior of the various bandwidth parameters as a function of γ for different maximum frequency (crosses correspond to $f_{\max} = 8f_{\mathrm{p}}$, triangles to $f_{\max} = 4f_{\mathrm{p}}$, circles to $f_{\max} = 3f_{\mathrm{p}}$).

This expression, based upon the statistical considerations discussed herein, provides a robust estimate of this parameter in a random sea state.

4. – Conclusions

In recent numerical experimental and theoretical work it has been bound that the Benjamin-Feir Index can play an important role for the determination of the statistical properties of the surface elevation of a random wave train. From a theoretical point of view this definition is unique only if a monochromatic wave is considered or if the

mathematical structure of the inverse scattering transform is invoked [7]. In the case of random waves, different methodologies for its computation are available, which of course would give different numerical estimations of the BFI. This of course could create some complications if the BFI of different experimental data needs to be compared. In order to overcome this difficulty we have performed a detailed study on the different possible methodologies that could be used. Our goal has been to determine a robust methodology, independent of the spectral resolution and of the cut-off frequency, that could be used directly from time (space) series or from frequency (wave number) spectra. We have focused our attention especially on the determination of the spectral bandwidth. Different methodologies are available for the estimation of the spectral bandwidth: we have considered the narrowness, the broadness and the peakedness parameters. Those methods have been applied to a JONSWAP spectrum and it was found that the most robust method is based on the peakedness parameter Q_{p}.

A second parameter important for the determination of the BFI is the spectral peak for which we have used the method proposed by Young.

The error on the estimate of the peak frequency and the spectral width does not exceed the 5% of the values, provided that the spectral resolution is lower than 0.15 times the peak frequency.

* * *

MO, MS and AO acknowledge support from MIUR.

REFERENCES

[1] Janssen P. A. E. M., *J. Phys. Ocean.*, **33** (2003) 863.
[2] Onorato M., Osborne A. R., Serio M. and Bertone S., *Phys. Rev. Lett.*, **86** (2001) 5831.
[3] Janssen P. A. E. M. and Bidlot J., R60.9/pj/0387 Memorandum Research Dept., ECMWF (2003).
[4] Mori N. and Yasuda T., *Rogue Wave 2000, Ifremer, Brest 29-30 November 2000*, edited by Olagnon M. and Athanassoulis G. A., pp. 229-244.
[5] Onorato M., Osborne A. R., Serio M., Cavaleri L., Brandini C. and Stansberg C. T., *Phys. Rev. E*, **70**, Art. No. 067302 (2004).
[6] Onorato M., Osborne A. R., Serio M. and Cavaleri L., *Phys. Fluids*, **17** (2005) 078101.
[7] Osborne A. R., Onorato M. and Serio M., *Proceedings of the 14th "Aha Huliko" a Winter Workshop ROGUE WAVES, Hawaij*, in press (2005).
[8] Mei C. C., in *The Applied Dynamics of Ocean Surface Waves* (John Wiley, New York) 2000, p. 615.
[9] Günther H., *Hamburger Geophys. Einzelsch*, **55** (1981) 1.
[10] Sobey R. J. and Young I. R., *ASCE J. Waterw. Port Costal Ocean Eng.*, **112** (1986) 370.
[11] Bishop C. T. and Donelan M. A., in *Civil Engineering Practice 3 - Geotechnical/Ocean Engineering* (Technomic Publ. Co. Inc., Lancaster, PA) 1988, pp. 653-695.
[12] Mansard E. P. D. and Funke E. R., *Proc. 22nd. Int. Coastal Eng. Conf., Delft, The Netherlands* (1990), pp. 465-477.
[13] Young I. R., *Ocean Eng.*, **22,** 7 (1995) 669.
[14] Goda Y., *Random Seas and Design of Marine Structures* (University of Tokyo Press) 1985, p. 239.
[15] Cartwright D. E. and Longuet-Higgins M. S., *Proc. R. Soc. London*, **237,** Issue 1209 (1956) 212.

[16] Longuet-Higgins M. S., *J. Geophys. Res.*, **86**(C5) (1975) 4299.
[17] Goda Y., *Rep. Port Harbour Res. Inst.*, **9** (1970) 3.
[18] Komen G. J., Cavaleri L., Donelan M., Hasselmann K., Hasselmann H. and Janssen P. A. E. M., *Dynamics and Modeling of Ocean Waves* (Cambridge University Press) 1994, p. 187.